



Green Approach to Corrosion Inhibition of Copper by Two Oils of *Argania Spinosa* (L.) in Phosphoric Acid

F. Mounir^{1,*}, S. El Issami¹, Lh. Bazzi², R. Salghi^{3,*}, N. Abidi⁴,
S. Jodeh⁵, L. Bazzi¹, A. Chihab Eddine⁶

¹ Laboratoire Matériaux et Environnement, Faculté des Sciences d'Agadir. Morocco.

² Etablissement Autonome de Contrôle et de Coordination des Exportations Agadir. Morocco.

³ Equipe de Génie de l'Environnement et de Biotechnologie, Université Ibn Zohr, ENSA, Agadir, Morocco.

⁴ Fiber and Biopolymer Research Institute, Department of Plant and Soil Science, Texas Tech University, Lubbock, Tx, USA.

⁵ Department of Chemistry, An-Najah National University, P. O. Box 7, Nablus, State of Palestine.

⁶ Laboratoire Chimie Organique, Faculté des Sciences d'Agadir. Morocco.

Received 8 Apr 2015, Revised 6 July 2015, Accepted 6 July 2015

*Corresponding author: E-mail: Fatiha MOUNIR: mounirfatiha@yahoo.fr and Rachid Salghi r.salghi@uiz.ac.ma

Abstract

The anti corrosion behaviour of Argan Oil (AO) and Cosmetic Argan Oil (CAO); extracted from *Argania spinosa* (L); in 2M H₃PO₄ containing 3.10-1 M NaCl solution on copper has been examined and characterized by weight loss, Tafel polarization, electrochemical impedance spectroscopy (EIS). The experimental results reveal that the oils were shown to have good inhibition efficiencies in phosphoric acid. EIS analysis revealed that increase in concentration increases the charge transfer resistance, thus increased inhibition efficiency. Potentiodynamic polarization studies showed the oils acted as a mixed-type of inhibitors. The adsorption mechanisms for both extracts were mainly physisorption. The results obtained from the various methods are in good agreement.

Keywords: Argan Oil; Cosmetic Argan Oil; corrosion; inhibition; copper.

1. Introduction

Copper and its alloys have many industrial applications such as electronics because of their excellent corrosion resistance properties as well as their superior electrical and thermal performance [1]. Most work on copper corrosion reveals that the presence of aggressive elements such as chloride and sulfide accelerates the corrosion of this metal[2–4]. One of the most important methods in the corrosion protection of copper is the use of organic inhibitors [5-7]. Inhibitors are substances or mixtures that in low concentration and in aggressive environment inhibit, prevent or minimize the corrosion[8]. Historically, inhibitors had great acceptance in the industries due to excellent anti-corrosive properties. However, many showed up as a secondary effect, damage the environment. Thus the scientific community began searching for friendly environmentally inhibitors, like the organic inhibitors[9-18], the present study investigates the inhibiting effect of *Argania spinosa* (L) oils, as safe corrosion inhibitors for the copper corrosion in 2M H₃PO₄ containing 3.10-1M NaCl solution. The chemical composition of Argan Oil and Cosmetic Argan Oil extracted from *Argania spinosa* (L) Skeels were Palmitic acid, Oleic acid, Linoleic acid, Schottenol, Spinasterol and γ -tocopherol (Table.1).

2. Materiels and Methodes

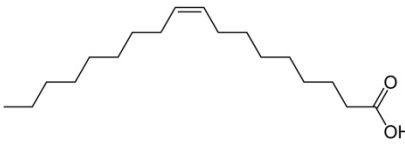
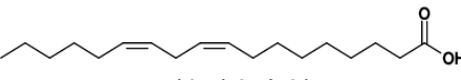
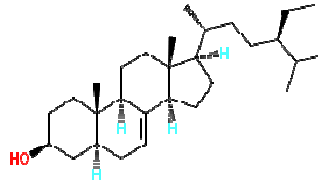
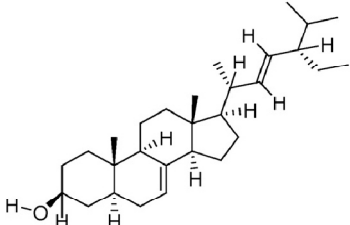
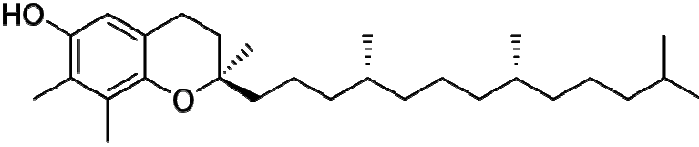
2.1. Weight loss measurements

Determination of weight loss of the coupons in a corrosion experiment is one of the common methods to calculate corrosion rates. Coupons were cut into 12 cm².

All experiments were carried out under total immersion in 75 ml of test solutions. Mass loss was recorded by an Analytical balance. Prior to each gravimetric or electrochemical experiment, the surface of the specimens was

polished successively with emery paper up to 1200 grade, rinsed thoroughly with acetone and bidistilled water before plunging the electrode in the solution. Pure copper samples (99%) were used. The experiments were carried out in 2 M H₃PO₄ medium containing 0,3 M of NaCl; it was prepared by dilution of Analytical Grade 84% H₃PO₄ with bidistilled water and pure NaCl.

Table 1. Chemical structure and pourcentage of the main constituents of *Argania spinosa* (*L.*) oils.

	 Linoleic Acid	
Oleic acid (C18:1) OA (45.1 %), COA (46.3 %)	Linoleic acid (C18:2) OA (34.5%), COA (32.3 %)	Schottenol OA (46 %), COA (48.4 %)
		
Spinasterol A (37 %), COA (39.1 %)	γ-tocopherol OA (85.1%), COA (86,9 %)	

2.2. Electrochemical tests

The electrochemical study was carried out using a potentiostat PGZ100 piloted by Voltmaster soft-ware. This potentiostat is connected to a cell with three electrode thermostats with double wall (Tacussel Standard CEC/TH). A saturated calomel electrode (SCE) and platinum electrode were used as reference and auxiliary electrodes, respectively. The working electrode is in the form of a disc from pure copper of the surface 1 cm² used as a work electrode that is mechanically abraded with 1200 grade of emery papers, rinsed with distilled water then with ethanol before plunging the electrode in the solution. The potential was stabilized at free potential during 30 min. The polarisation curves are obtained from -800 mV to 500 mV at 298 K. In order to investigate the effects of temperature and immersion time on the inhibitor performance were carried out in a temperature range 298–328 K.

The electrochemical impedance spectroscopy (EIS) measurements are carried out with the electrochemical system (Tacussel), which included a digital potentiostat model Voltalab PGZ100 computer at E_{corr} after immersion in solution without bubbling. After the determination of steady-state current at a corrosion potential, sine wave voltage (10 mV) peak to peak, at frequencies between 100 kHz and 10 mHz are superimposed on the rest potential. Computer programs automatically controlled the measurements performed at rest potentials after 0.5 hour of exposure at 298 K. The impedance diagrams are given in the Nyquist representation. Experiments are repeated three times to ensure the reproducibility.

3. Results and Discussions

3.1. Gravimetric study

Table 2 resumes obtained in 2M H₃PO₄ containing 3.10⁻¹ M NaCl (X_{corr}) and at various contents of AO and CAO (X'_{corr}) determined at 298 K after 8 h of immersion rate and inhibition efficiencies E_w, determined by the relation:

$$E_w(\%) = \frac{X_{\text{corr}} - X'_{\text{corr}}}{X_{\text{corr}}} \times 100 \quad (1)$$

where X_{corr} and X'_{corr}, are the corrosion rates of copper with and without AO and CAO inhibitors, respectively.

Tableau 2: Copper weight loss data and inhibition efficiency of CAO and AO in 2 M H₃PO₄ + 0,3 M NaCl.

Concentration (g/l)	Inhibitors	W' _{corr} (mg.j ⁻¹ . dm ⁻²)	E _w (%)
0	Blank	162	-
1	CAO	62	62
	AO	79	51
2	CAO	50	69
	AO	70	57
5	CAO	26	84
	AO	52	68
6	CAO	16	90
	AO	44	73
7	CAO	3	98
	AO	13	92

It can be seen from Table 2 that both green inhibitors showed efficient anticorrosive property copper in 2M H₃PO₄ + 0,3 M NaCl aggressive media. It is noted that inhibition efficiencies increases with the increase of inhibitors concentration. This may be due to the increase in adsorption of more phytomolecules at the metal/solution interface on increasing the concentration of inhibitors. The increase in inhibition efficiencies was noticed until the inhibitors concentration reached up to 7g/L .

3.2. Polarization curves

Typical potentiodynamic polarization curves for copper in 2M H₃PO₄ + 3.10⁻¹ M NaCl in the presence and absence of the selected inhibitors (CAO and AO) at 7 g/L is shown in Fig.1-5. Electrochemical corrosion kinetics parameters, i.e. corrosion potential (E_{corr}), cathodic and anodic Tafel slopes (β_c , β_a), corrosion current density (I_{corr}) obtained from the Tafel extrapolation of the polarization curves and (E%) are given in Table 3.

The E% was calculated by using the following equation :

$$E\% = \left(1 - \frac{I_{corr}}{I'_{corr}}\right) \times 100 \quad (2)$$

Where I_{corr} and I'_{corr} are the corrosion current density without and with addition of the inhibitors, respectively.

Table 3. Electrochemical parameters of copper at various concentrations of AO and CAO in 2M H₃PO₄ + 0,3 M NaCl and corresponding inhibition efficiency.

concentration	Inhibitors	E _{corr} (mV/SCE)	I _{corr} (μA/cm ²)	b _a (mV/dec)	b _c (mV/dec)	IE (%)
0	Blank	-177	36	68	-297	--
1 g/l	CAO	-192	14	69	-487	61
	AO	-179	17	62	-350	53
2 g/l	CAO	-192	21	68	-462	67
	AO	-176	14	63	-350	61
5 g/l	CAO	179	7	67	-486	81
	AO	-210	10	69	-415	72
6 g/l	CAO	-191	4	71	-401	89
	AO	-209	6	71	-350	84
7 g/l	CAO	-195	2	69	-471	95
	AO	-207	2	58	-407	94

The examination of Figs.1- 5 and Table 3 shows the anodic and cathodic polarization curves of copper in 2M $H_3PO_4 + 0,3 M NaCl$ solution, without and with AO and CAO at $25 \pm 1 C$ after immersion for 30 min. It is observed that both the cathodic curves and anodic curves show lower current density in the presence of the inhibitors than those recorded in the solution without inhibitors. This indicates that AO and CAO inhibit the corrosion process. The results of Figs.1- 5 also clearly illustrate the fact that AO and CAO, under the studied conditions, brings down the corrosion current without causing any considerable change in the corrosion mechanism, suggesting that the studied AO and CAO are of mixed-type inhibitors.

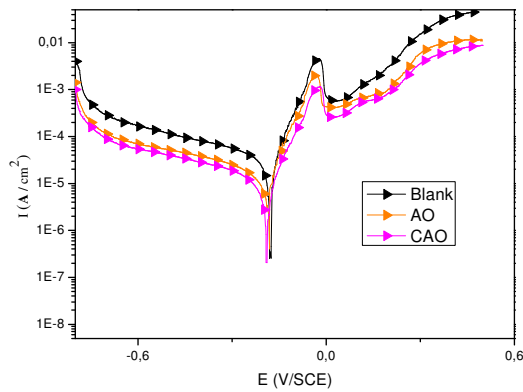


Figure 1. Cathodic and Anodic polarisation curves of copper in (2M $H_3PO_4 + 0.3 M NaCl$) at **1 g/L** of AO and CAO

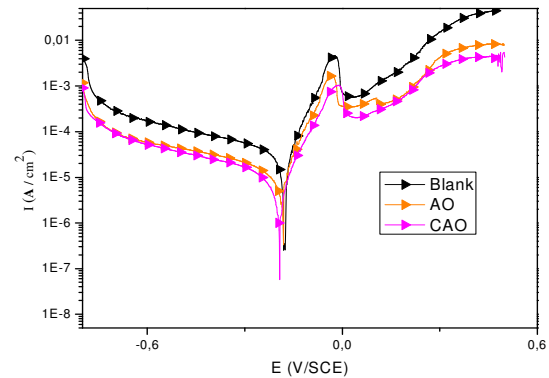


Figure 2. Cathodic and Anodic polarisation curves of copper in (2M $H_3PO_4 + 0.3 M NaCl$) at **2 g/L** of AO and CAO

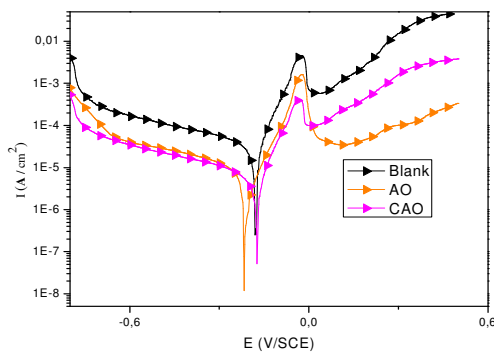


Figure 3. Cathodic and Anodic polarisation curves of copper in (2M $H_3PO_4 + 0.3 M NaCl$) at **5 g/L** of AO and CAO.

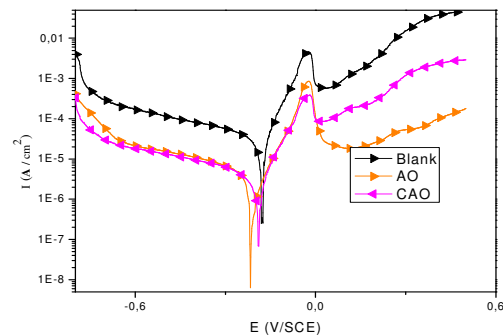


Figure 4. Cathodic and Anodic polarisation curves of copper in (2M $H_3PO_4 + 0.3 M NaCl$) at **6 g/L** of AO and CAO.

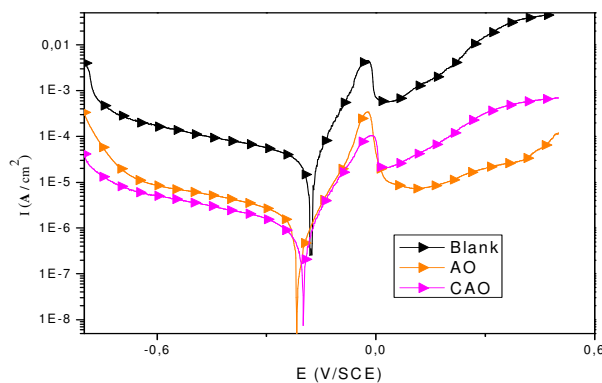


Figure 5. Cathodic and Anodic polarisation curves of copper in (2M $H_3PO_4 + 0.3 M NaCl$) at **7 g/L** of AO and CAO.

The inhibition efficiency reaches 95% and 94 % at 7g/L of AO and CAO, respectively. This phenomenon is interpreted by the adsorption of the molecules on copper surface leading to the increase of the surface coverage θ defined by $IE(\%) / 100$. $IE(\%)$ increases with compound concentration. We may conclude that AO and CAO are effective inhibitors of copper corrosion in 2M $H_3PO_4 + 0,3 M NaCl$.

It is observed that the results of surface coverage in presence of the selected inhibitors (AO and CAO) are in good agreement with those given by weight loss technique. This means that the inhibition efficiency calculated with the help of galvanostatic polarisation technique are nearly equal to the values obtained by weight loss technique.

3.3. Electrochemical impedance spectroscopy results

Corrosion behaviour of copper, in (2M $H_3PO_4 + 0,3 M NaCl$) solution with and without argan oils at different concentrations after immersion for 30 min is investigated by electrochemical impedance spectroscopy (EIS) measurements at 298 K. The corresponding Nyquist diagram are shown in Figs. 6-10.

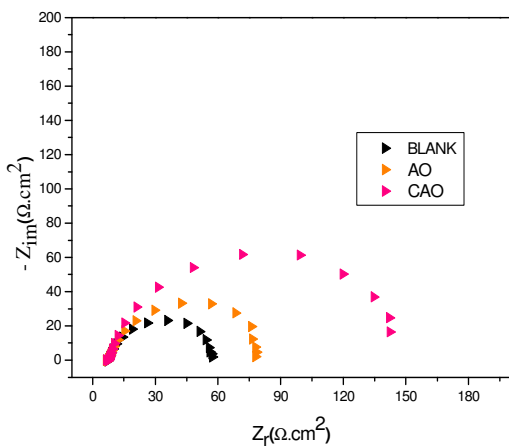


Figure 6. Nyquist diagrams for copper electrode in (2M $H_3PO_4 + 0,3M NaCl$) with and without **1 g/L** of inhibitor after 30min of immersion at E_{corr} .

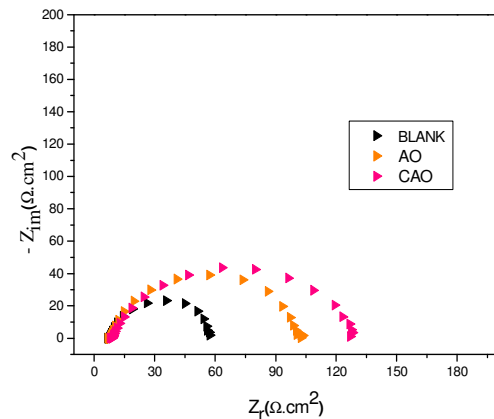


Figure 7. Nyquist diagrams for copper electrode in (2M $H_3PO_4 + 0,3M NaCl$) with and without **2 g/L** of inhibitor after 30min of immersion at E_{corr} .

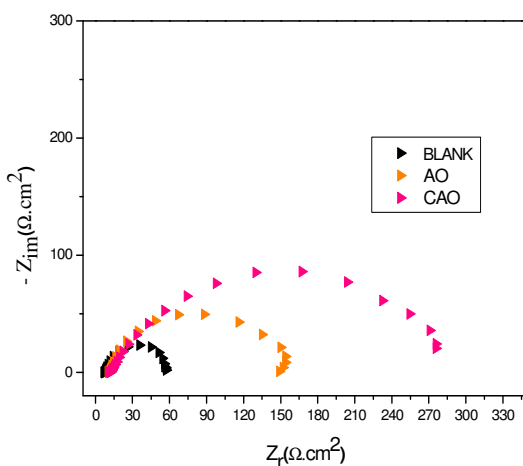


Figure 8. Nyquist diagrams for copper electrode in (2M $H_3PO_4 + 0,3M NaCl$) with and without **4 g/L** of inhibitor after 30min of immersion at E_{corr} .

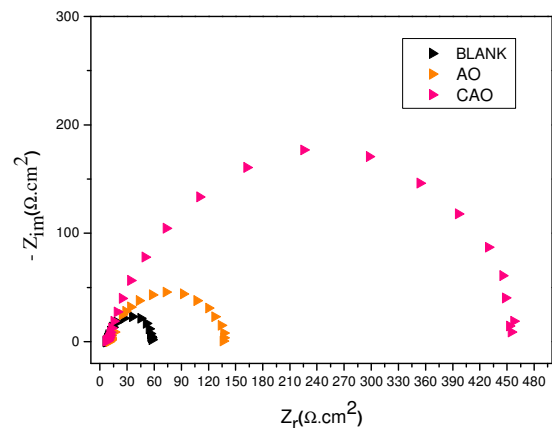


Figure 9. Nyquist diagrams for copper electrode in (2M $H_3PO_4 + 0,3M NaCl$) with and without **6 g/L** of inhibitor after 30min of immersion at E_{corr} .

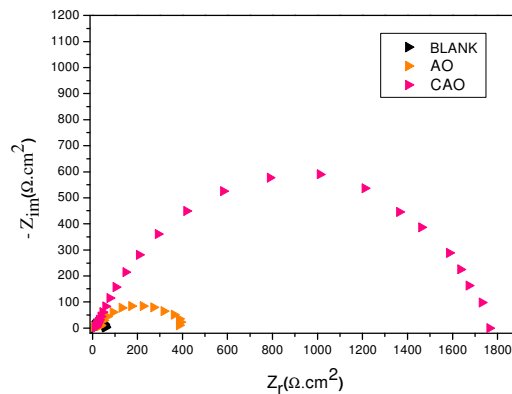


Figure 10. Nyquist diagrams for copper electrode in (2M H₃PO₄+ 0,3M NaCl) with and without 7 g/L of inhibitor after 30min of immersion at E_{corr}.

The values of inhibition efficiency were calculated using the relation:

$$E_{Rt} \% = \frac{(R_t - R_t^0)}{R_t} \times 100 \quad (3)$$

Where R_t and R_t^0 are the charge transfer resistances in inhibited and uninhibited solutions respectively. The charge transfer resistance (R_t) values are calculated from the difference in impedance at lower and higher frequencies, as suggested by Tsuru et al [19]. The double layer capacitance (C_{dl}) and the frequency (f_{max}) at which the imaginary component of the impedance is maximal ($-Z_{max}$) are found as represented in equation:

$$C_{dl} = \left(\frac{1}{\omega \cdot R_t} \right) \quad (4)$$

Where $\omega = 2\pi f_{max}$

with C_{dl} : Double layer capacitance ($\mu\text{F}\cdot\text{cm}^{-2}$); f_{max} : maximum frequency (Hz) and R_t : Charge transfer resistance ($\Omega\cdot\text{cm}^2$)

Table 4. Impedance parameters for corrosion of copper in (2M H₃PO₄+ 0,3 M NaCl) at various concentrations of CAO and AO .

concentration	Inhibitors	R_t ($\Omega\cdot\text{cm}^2$)	f_{max} (Hz)	C_{dl} ($\mu\text{F}/\text{cm}^2$)	E_{Rt} (%)
0	Blank	51	63	49	--
1 g/l	CAO	141	40	28	64
	AO	100	45	35	50
2 g/l	CAO	152	38	27	67
	AO	121	44	30	59
5 g/l	CAO	281	22	25	82
	AO	150	40	26	67
6 g/l	CAO	460	15	23	89
	AO	180	39	23	72
7 g/l	CAO	1755	11	08	97
	AO	400	23	10	88

The values of f_{max} , C_{dl} and the charge transfer resistances R_t were presented in Table 4. We can see that, the R_t value increases with increasing concentration of inhibitors in 2M H₃PO₄+ 0,3 NaCl solution, whereas C_{dl} decreases. This suggests that the copper surface coverage increases with inhibitors concentrations. The capacitance value C_{dl} is about 49 $\mu\text{F}/\text{cm}^2$ in the absence of inhibitors and 08 $\mu\text{F}/\text{cm}^2$

and $10\mu\text{F}/\text{cm}^2$ in the presence of CAO and AO respectively at 7 g/L (Table 4). The decrease of the capacitance can be explained by a reduction of the active metal surface, which is probably due to the species adsorption or to the development of compounds on the surface [20]. The inhibition efficiency, calculated from impedance spectra at free potential in the presence of inhibitors at various concentrations, is presented. This inhibition efficiency increases when the inhibitors concentrations increase. Inhibition efficiency values exceed of AO and CAO respectively are 88 % and 97% at 7g/L. This confirms the results obtained by potentiodynamic and gravimetric tests.

3.4. Effect of temperature and thermodynamic activation parameters

Being given that the temperature is one of the factors that may affect the behavior of a material in a corrosive environment, and can also modify the metal-inhibitor interaction, it is essential to study the effect of this factor on the protection rates, as well to determine the mechanism of inhibition.

The study of the influence of temperature on the rate of corrosion inhibition of copper by our inhibitors were performed at temperatures 298K - 323K in the absence and in the presence of inhibitor at 7g/L (Figs. 11-14). This study to determine the activation energies, enthalpies and entropies of activation of the corrosion process and thus provides information on the mechanism of inhibition. The corresponding data are shown in Table 5.

Table 5. Effect of temperature on the copper in (2M H_3PO_4 + 0,3 M NaCl) and at 7g/L of AO and COA.

Temperature (K)	Inhibitors	E_{corr} (mV/SCE)	I_{corr} ($\mu\text{A}/\text{cm}^2$)	b_a (mV/dec)	b_c (mV/dec)	E (%)
298	Blank	-177	36	68	-297	-
	CAO	-195	02	69	-417	95
	AO	-217	02	41	-407	94
303	Blank	-157	116	63	-516	-
	CAO	-176	18	53	-498	84
	AO	-216	14	75	-427	87
313	Blank	-136	174	54	-504	-
	CAO	-174	47	64	-354	73
	AO	-197	40	89	-341	77
323	Blank	-128	251	50	-355	-
	CAO	-175	83	59	-509	68
	AO	-193	76	62	-430	71

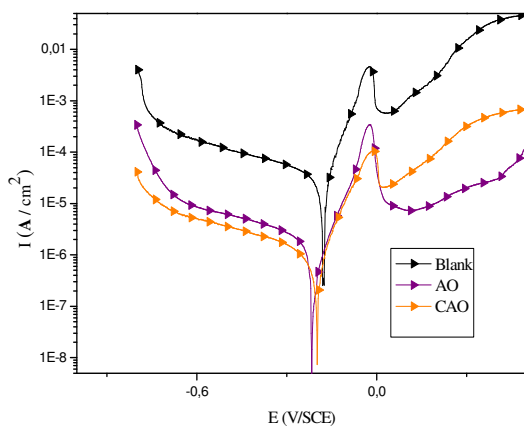


Figure. 11 Potentiodynamic polarisation curves of copper in (2M H_3PO_4 + 0.3 M NaCl) with and without 7 g/L of inh. at 298 K.

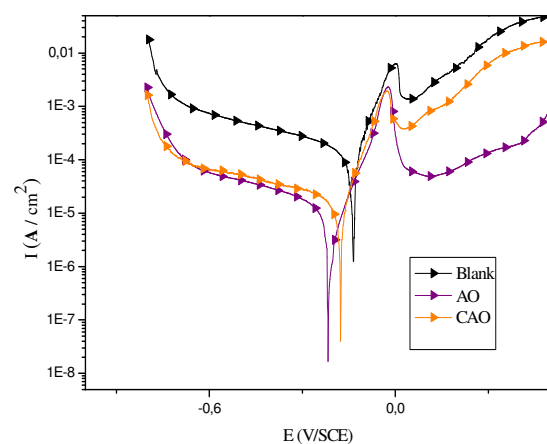


Figure. 12 Potentiodynamic polarisation curves of copper in (2M H_3PO_4 + 0.3 M NaCl) with and without 7 g/L of inh. at 303 K.

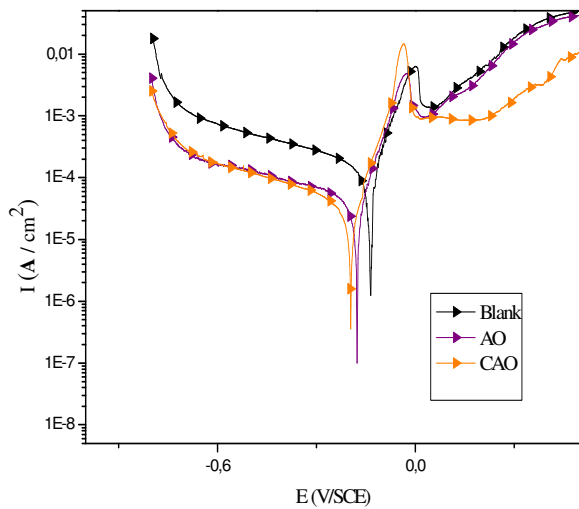


Figure. 13 Potentiodynamic polarisation curves of copper in (2M H₃PO₄ + 0.3 M NaCl) with and without 7 g/L of inh. at 313 K.

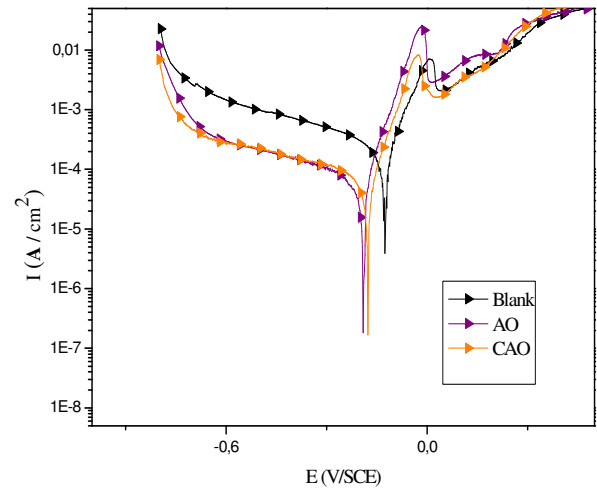


Figure. 14 Potentiodynamic polarisation curves of copper in (2M H₃PO₄ + 0.3M NaCl) with and without 7 g/L of inh. at 323 K.

From these results, we can deduce that the corrosion rate increases in the blank with the rise of temperature. In the presence of AO and CAO I_{corr} is highly reduced. Also, the inhibition efficiency decreases slightly with increasing temperature. This can be explained by the decrease of the strength of adsorption processes at elevated temperature and suggested a physical adsorption mode [21,22]. From this result, we can conclude that AO and CAO are excellent inhibitors.

The activation energy can be determined from the Arrhenius plots for copper corrosion presented in Fig. 15 by using the following relations:

$$I_{corr} = A \cdot \exp\left(-\frac{E_a}{R \cdot T}\right) \quad (5)$$

Where:

A: Arrhenius factor

E_a : Apparent activation corrosion energy

R: Perfect gas constant

T: Absolute temperature.

Plotting ($\log I_{corr}$) versus $1/T$ gives straight lines as revealed from Fig. 15.

$$I_{corr} = \frac{RT}{Nh} \cdot \exp\left(\frac{\Delta S^*}{R}\right) \cdot \exp\left(-\frac{\Delta H^*}{RT}\right) \quad (6)$$

Where :

N :Avogadro's number,

h :Plank's constant,

R : Perfect gas constant,

ΔS^* and Entropy of activation

ΔH^* : Enthalpy of activation.

Fig.16 shows a plot of $\ln(I_{corr}/T)$ against $1/T$ for CAO and AO. Straight lines are obtained with a slope of $(-\Delta H^*/R)$ and an intercept of $(\ln R/Nh + \Delta S^*/R)$ from which the values of ΔH^* and ΔS^* are calculated respectively (Table 6).

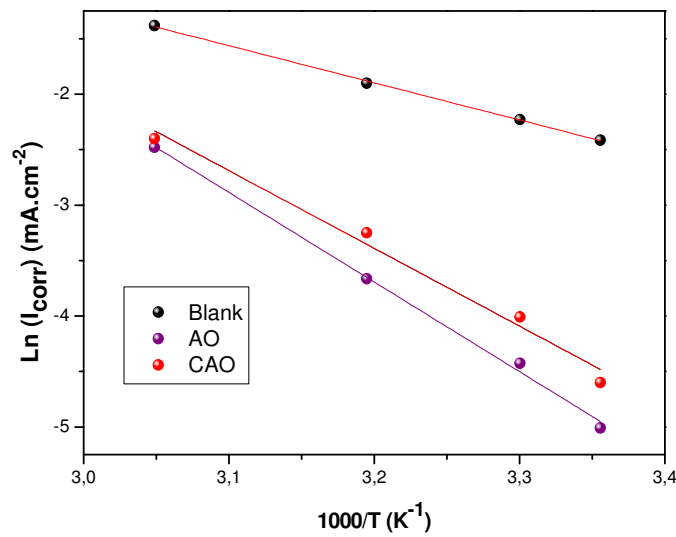


Figure 15. Arrhenius plots of copper in (2M H₃PO₄ + 0,3 M NaCl) with and without 7 g/L of CAO and AO.

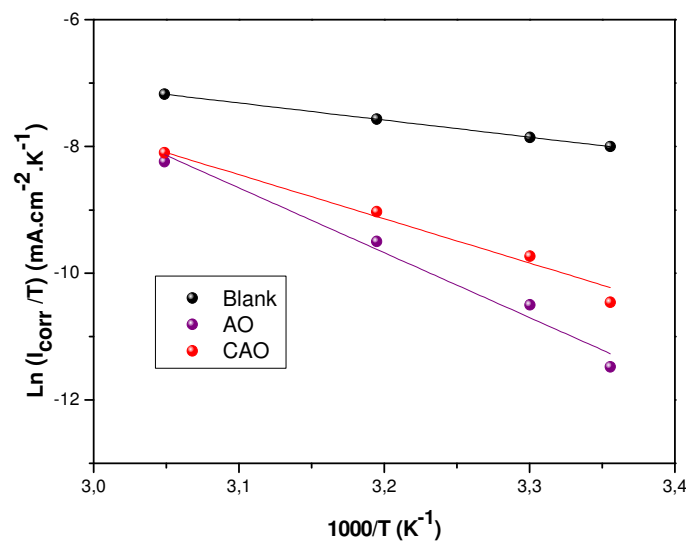


Figure.16 Relation between $\text{Ln}(I_{\text{corr}}/T)$ and $1000/T$ at different temperatures.

The E_a , ΔH^* and ΔS^* values were determined from the slopes of these plots. The calculated values of E_a , ΔH^* and ΔS^* in the absence and the presence of 7 g/L of OA and COA are given in table 6.

Table 6. The value of activation parameters for copper in 2M H₃PO₄ + 0,3 M NaCl in the absence and presence of 7 g/L of OA and COA .

	$E_a(\text{kJ/mol})$	$\Delta H^*(\text{kJ/mole})$	$\Delta S^*(\text{J.mole}^{-1}.\text{k}^{-1})$
Blank	50	48	-111
COA	95	92	-019
AO	99	94	-010

Inspection of these data reveals that the apparent activation energy E_a in 2M H₃PO₄ + 3.10⁻¹M NaCl solution in the absence of the inhibitors was 50 kJ/mol. The addition of inhibitors to the acid solution increases the

activation energy. The positive sign of enthalpies reflect the endothermic nature of copper dissolution process meaning that dissolution of copper is difficult [23]. On comparing the values of the entropy of activation ΔS^* a given in Table (6), it is clear that entropy of activation increased positively in the presence of inhibitors than in the absence of inhibitors. The increase ΔS^* of a reveals that an increase in disordering takes place on going from reactant to the activated complex [24].

Conclusion

The following results can be drawn from this study:

- ❖ AO and CAO act as mixed type inhibitors.
- ❖ The inhibition efficiency of AO and CAO increases with the rise of inhibitors concentration.
- ❖ The data obtained from the different methods: potentiodynamic polarization, EIS and weight loss measurements are in good agreement.
- ❖ AO and CAO are excellent inhibitors for copper in acidic medium at 298K.
- ❖ AO and CAO natural and environmentally benign products they can be used as an alternative for toxic chemical inhibitors in acidization and acid pickling of copper.

References

1. Leidheiser H., Robert E., Krieger Publishing Company, Huntington, NY, (1979) 71 – 126.
2. Charles J., Catelin D., Dupoirion F., *Mater. Technol* 8 (1987) 309.
3. Sedrik A.J., *Corrosion* 42 (1986) 376.
4. Nassif N., *Surf. Technol* 26 (1985) 189.
5. Zhang D.Q., Gao L.X., Zhou G.D., *Appl. Surf. Sci* 225 (2004) 287.
6. Zhang D.Q., Gao L.X., Zhou G.D., *Corros. Sci.* 46 (2004) 3031.
7. Zhang D.Q., Gao L.X., Zhou G.D., *J. Appl. Electrochem* 33 (2003) 361.
8. Obot I.B., Obi-Egbedi N.O., Umoren S.A., *Corros. Sci.* 51 (2009) 1868-1875.
9. Negm A. N., Kandile N. G., Badr E. A., Mohammed M. A., *Corrosion Science* 65 (2012) 94-103.
10. Abdel-Gaber A. M., Abd-El-Nabey B.A., Khamis E., Abd-El-Khalek D.E., *Desalination* 278 (2011) 337-342.
11. Salasi M., Sharabi T., Roayaei E., Aliofkhazraei M., *Materials Chemistry and physics* 104 (2007) 183-190.
12. Blustein G., Romagnoli R., J.A. J. *Colloids and Surfaces A: Physicochemical and Engineering Aspects* 290 (2006) 7-18.
13. Bommersbach P., Alemany-Dumont C., Millet J.P., Normand B., *Electrochimica Acta* 51 (2005) 1076-1084.
14. Lecante A., Robert F., Blandinières P.A., C. Roos. *Current Applied Physics* 11 (2011) 714-724.
15. Radojčić, Berković K., Kovač S., Vorkapić-Furač J., *Corrosion Science* 50 (2008) 1498-1504,
16. Okafor P.C., Ikpi M.E., Uwah I.E., Ebenso E.E., Ekpe U.J., Umoren S.A., *Corrosion Science* 50 (2008) 2310-2317.
17. Mounir F., El Issami S., Bazzi Lh., Chihab Eddine A., Belkhaouda M., Bammou L., Salghi R., Jbara O., Bazzi L., *JCBPAT* 4 (2014) 2249 –1929.
18. Mounir F., El Issami S., Bazzi Lh., Jbara O., Chihab Eddine A., Belkhaouda M., Bammou L., Salghi R., Bazzi L., *Mor. J. Chem.* 2 (2014) 33-45.
19. Tsuru T., Haruyama S., Gijutsu B., Jpn J., *Soc. Corros. Eng* 27 (1978) 573.
20. Bouklah. M., Hammouti. B., Lagrenée. M., Bentiss. F. *Corros. Sci* 48 (2006) 2831-2842.
21. Popova A., Sokolova E., Raicheva S., Christov M., *Corros. Sci* 45 (2003) 33.
22. Szauer T., Brandt A., *Electrochim. Acta* 22 (1981) 1209.
23. Guan N. M., Xueming L., Fei L., *Mater. Chem. Phys* 86 (2004) 59-68.
24. Bentiss F., Traisnel M., Lagrenée M., *Corros. Sci* 47 (2005) 2915-2931.

(2015) ; <http://www.jmaterenvirosci.com>